Terahertz Emission and Detection Using Two Dimensional Plasmons in Semiconductor Nano-Heterostructures for Sensing Applications

Taiichi Otsuji, Takayuki Watanabe,
Stephane Boubanga Tombet, Tetsuya Suemitsu,
Victor Ryzhii
Research Institute of Electrical Communication
Tohoku University
Sendai, Japan
otsuji@riec.tohoku.ac.jp

Vyacheslav Popov
Kotelnikov Institute of Radio Engineering and Electronics
(Saratov Branch)
Russian Academy of Sciences
Saratov, Russia

Wojciech Knap
L2C Laboratories
University of Montpellier-CNRS
Montpellier, France

***Abstract*—This paper reports on emission and detection of terahertz radiation using two dimensional (2D) plasmons in semiconductor nano-heterostructures for sensing applications. The device structure is based on a high-electron mobility transistor and incorporates the authors' original asymmetrically interdigitated dual-grating gates. Excellent terahertz emission and detection performances are experimentally demonstrated by using InAlAs/InGaAs/InP heterostructure material systems. Their applications to nondestructive material evaluation based on terahertz imaging are also presented.**

I. Introduction

Two-dimensional (2D) plasmons in submicron transistors have attracted much attention due to their nature of promoting emission and detection of electromagnetic radiation in the THz range. Coherent plasmonic THz emission can be made by the plasma wave instabilities described by the Dyakonov–Shur (D-S) Doppler-shift model [1] and/or Ryzhii-Satou-Shur (R-S-S) transit-time model [2], but suffering from incoherent broadband emission at 300K. On the other hand, hydrodynamic nonlinearities of 2D plasmons in high-electron-mobility transistors (HEMTs) are promising for fast and sensitive rectification/detection of THz radiation [3], but exhibiting a poor sensitivity in case of grating-gate-type broadband antenna structures. This paper reports on emission and detection of THz radiation using 2D plasmons in semiconductor nano-heterostructures for sensing applications. The device structure is based on a high-electron mobility transistor and incorporates the authors' original asymmetrically interdigitated dual-grating gates. Excellent THz emission and detection performances are demonstrated by using InP-based heterostructure material systems. Their THz sensing applications are also presented.

This work was supported by JST-ANR WITH, Japan and France, JSPS-RFBR JPN-RUS joint program, Japan and Russia, and RFBR, Russia.

II. Asymmetric Dual-Grating-Gate THz Emitters

A. Device structure and principle of operation

In order to realize coherent monochromatic THz emission we introduced our original asymmetric dual-grating-gate (A-DGG) structure (Figs. 1) [4]. In the A-DGG structure the DGG is implemented with asymmetric inter-finger spaces. THz electric field distribution and resultant photoresponse were numerically simulated using a self-consistent electromagnetic approach combined with the perturbation theory for the hydrodynamic equations for 2D plasmons in HEMTs under periodic electron density modulation conditions [4]. Figure 2(a) shows giant enhancement of the responsivity (by four orders of magnitude) in an A-DGG HEMT under drain-unbiased conditions with respect to that for a symmetric DGG (S-DGG) HEMT for a dc drain bias current density of 0.1 A/m. When the A-DGG HEMT is dc-drain biased, the asymmetry of the plasmonic cavity is enhanced enormously as shown in Fig. 2(b), resulting in further enhancement of the responsivity by orders of magnitude. It is reasonable to suggest that similar enhancement should be also exhibited for the plasmon instability of the D-S type in the A-DGG HEMT. A chirped DGG structure was also introduced in order to uniform the plasmon frequencies over the entire DGG area under a specific drain-source bias V_{ds} condition that can promote the instability. These two features are combined to serve an asymmetric chirped (AC) DGG structure. Moreover, high-Q vertical photonic cavity structure is installed as shown in Fig. 1 to stimulate the coherent plasmon excitation [5].

978-1-4673-4642-9/13/$31.00 ©2013 IEEE

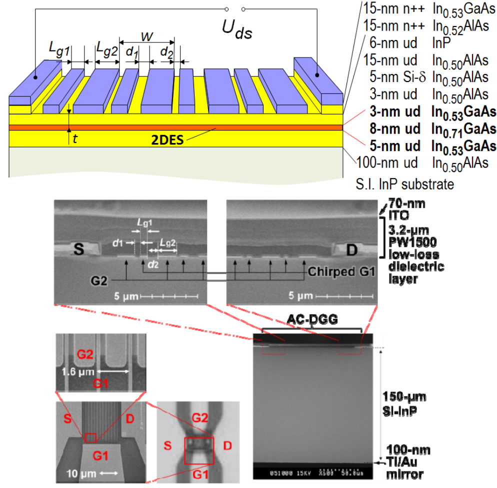

Figure 2. Schematic view and scanning electron micrographic images of an AC-DGG HEMT THz emitter/detector.

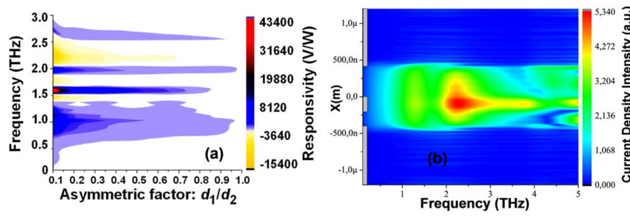

Figure 3. (a) Simulated relative responsivity as a function of d_1/d_2. L_{g1} = 400 nm, L_{g2} = 2.4 μm, $d_1 + d_2$ = 800 nm, W = 3.6 μm. Electron density under G2: 2.5×10^{11} cm^{-2}, and that the other area: 2.5×10^{12} cm^{-2}. (b) Simulated current distribution underneath a unit A-DGG cell for the assymetric factor of $d_1/d_2 = 0.5$

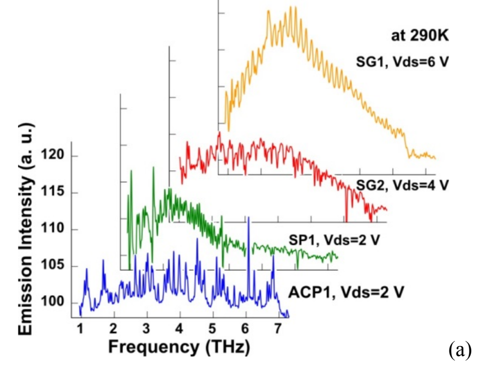

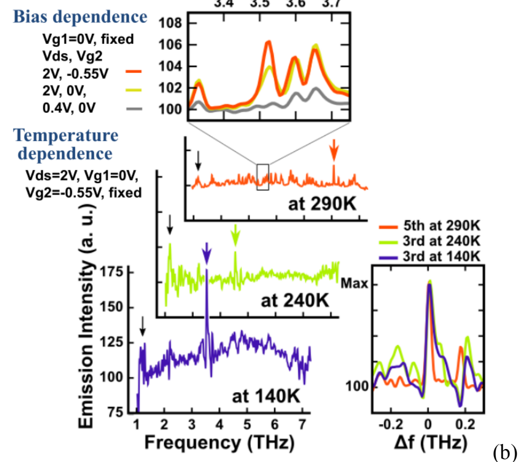

Figure 1. (a) Measured emission spectra at 290K for different material systems and DGG structures. Sample ACP1 is the AC-DGG. Samples SP1, SG1, and SG2 are S-DGGs.(after [5]) (b) Measured emission spectra at different biases at 290K (upper) and at different temperatures at optimal bias conditions (V_{ds} = 2 V, V_{g1} = 0 V, V_{g2} = -0.5 V) (lower) of sample ACP1 (InP-based AC-DGG HEMT). Arrows designates the 1st, 2nd, and 3rd plasmon modes. Inset magnifies the spectral portions of the 3rd and 5th mode. (after [7].)

B. Eperimental results and discussion

AC-DGG HEMTs were designed and fabricated using InAlAs/InGaAs/InP materials (see Fig. 1) [5]. Two grating gates G1 and G2 were formed with 70-nm thick Ti/Au/Ti by a standard lift-off process. Asymmetric factor, the ratio of the inter-finger spaces, d_1/d_2, was fixed to be 0.5. The grating gates G1 with narrower fingers L_{g1}, serving plasmon cavity gates, were designed to be chirped ranging from 215 to 430 nm. After processing the AC-DGG HEMT, a high-Q vertical cavity with a high finess of ~60 was formed with a 4.4-μm thick transparent PW1500 resist as a low-loss buffer layer and a 70-nm thick ITO mirror coat on top and a 100-nm Ti/Au coat on polished back surface (see Fig. 1(b)). Its fundamental resonant frequency (free spectral range of the Fabry-Perot modes) was designed to be 65 GHz.

The fabricated HEMTs exhibit normal dc transfer characteristics with good pinch-off and gate modulations for both G1 and G2 with threshold levels of -1.1 and -0.9 V, respectively. We conducted THz spectroscopic measurements for the fabricated devices using a Fourier-transform far-infrared spectrometer and a 4.2-K-cooled Si composite bolometer. The gate bias for the plasmon cavities V_{g1} was fixed at 0 V. Material- and structure-dependent emission spectra at 290K are plotted in Fig. 3(a) in comparison with previously reported GaAs-based and InP-based symmetric DGG HEMTs [6]. The drain bias V_{ds} was set so as to equalize the voltage drop along a unit DGG section among all the devices. Superiorities of the A-DGG structure and InP based materials with higher electron mobility (~11,000 cm^2/(Vs)) reflects intense background-less emission of Fabry-Perot-modes. The highest peak intensity is observed at ~6.2 THz with a sharp linewidth ~1.23 cm^{-1} (~37 GHz) corresponding to the 5th plasmon mode. Figure 3(b) plots the bias and temperature dependencies of measured emission spectra for an AC-DGG type sample ACP1. As a bias dependence, by increasing V_{ds} the whole emission intensity of Fabry-Perot modes raises, reflecting the hot-plasmon-originated broadband background emission. Furthermore, by applying appropriate biases for DGG: V_{g1} of 0 V and V_{g2} of -0.55 V to make a strong contrast on the electron densities on plasmonic cavities the peak at ~3.55 THz is enhanced, reflecting the 3rd harmonics of the plasmon resonance driven by the D-S type instability. At lower temperatures electron momentum relaxation times increase and hot-plasmon background is suppressed, resulting in more intense monochromatic coherent emission at ~3.55 THz corresponding to the 3rd plasmon

mode matched to a Fabry-Perot mode at 140K. Such phenomena are interpreted as a stimulated superradiant THz emission originated from cooperative promotion of D-S and R-S-S plasmon instabilities with hot-plasmons' spontaneous background emission. The output power of sample ACP1 is estimated to be of the order of 0.1 to 1 μW. Further increase in the asymmetric factor of the AC-DGG will lead to monochromatic THz oscillations at room temperature.

III. A-DGG HEMT THz Detectors

A. *Device structure and principle of operation*

The hydrodynamic motion of the plasma waves yields a nonlinear plasma-wave current component as the product of the local electron density and local electron velocity both of which are perturbed by incoming THz radiation, giving rise to quadratic rectification component in the current time-integral. This is the fundamental principle of the THz detection using the plasma-wave dynamics [3]. In an open-drain and source-terminated asymmetric boundary condition the generated (rectified) photocurrent is transformed to a dc voltage component leading to photovoltaic signal at the drain terminal.

As mentioned in section II, the A-DGG structure can provide ultra-high sensitive THz detection [4]. This is because the unit cell of the A-DGG structure can create strong build-in asymmetric electric field. The THz photoresponse dramatically increases when the parts of 2D channel under the fingers of one of the two sub-gratings are depleted. The device under characterization is identical to the InAlAs/InGaAs/InP A-DGG HEMTs shown in Fig. 1 except for uninstalling the vertical cavity.

B. *Eperimental results and discussion*

We conducted room temperature THz photovoltaic measurements with the fabricated detectors. Monochromatic THz pulsed waves with frequencies from 1 to 3 THz from a ring-cavity THz parametric oscillator source are focused on the detector [8-10]. The photovoltaic signal was observed as a V_{ds} variation with a lock-in technique. The responsivity was estimated as $R_v = \Delta U \cdot S_t / P_t \cdot S_d$ where ΔU is the THz-radiation-induced dc drain voltage, P_t is the total power of the THz beam on the detector plane, S_t is the radiation beam spot area, and S_d is the active area of the detector.

Figure 4(a) shows the measured responsivity of the detector sample at 1 THz under zero-V_{ds} condition as a function of gate voltage swing ($V_{g1,2}$ - V_{th}); dc voltage of G1: V_{g1} (G2: V_{g2}) is swept while V_{g2} (V_{g1}) is floated (biased at 0 V) [8, 9]. The best result with R_v = 2.2 kV/W was obtained when sweeping V_{g1} to the threshold V_{th}. Figure 4(b) shows the measured responsivity of detector # at 1.5 THz under V_{ds}-biased conditions. With increasing V_{ds} from 0 to 0.4 V, the maximum responsivity increases up to 6.4 kV/W. All these values are, to the best of authors' knowledge, the best ever reported at these frequencies over any fast-response detector at 300K [10].

Figure 5 shows noise equivalent power (NEP) for a AC-DGG type detector ACP1 as a function of $V_{g1,2}$ under drain-unbiased condition [8]. The detector exhibits extremely low

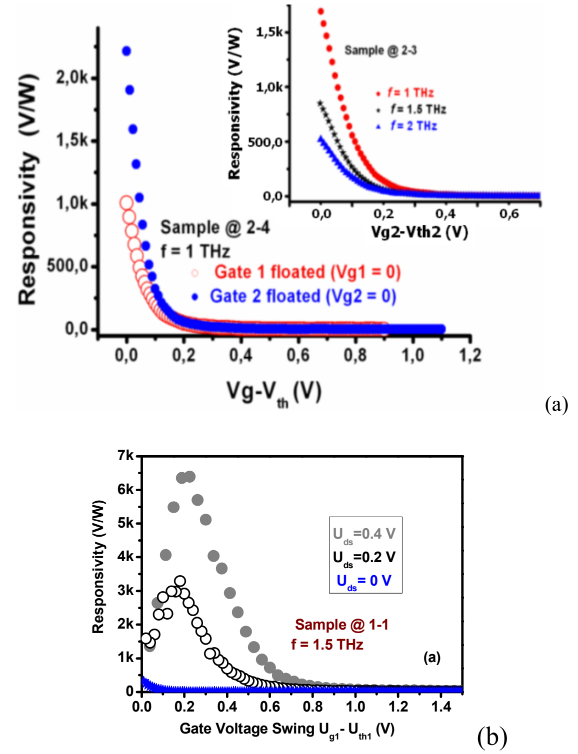

Figure 4. (a) Responsivity of detector # 2-4 as a function of the gate swing voltage (V_{g1} - V_{th1} or V_{g2} - V_{th2}) at 1 THz under drain-unbiased condition. The inset: responsivities of detector # 2-3 at 1, 1.5, and 2 THz as a function of the gate swing voltage V_{g2} - V_{th2} when G1 is floated. The responsivities become higher with lowering the gate voltages (taking the maximum at the threshold). (after [8]) (b) Responsivity of detector # 1-1 as a function of the gate swing voltage at 1.5 THz radiation under drain-biased conditions. (after [10])

NEP with the minimal value 15 pW/Hz$^{0.5}$ at 1 THz. These values are lower than those of any commercial room temperature THz detectors such as Golay cells (200 pW/Hz$^{0.5}$) or Schottky barrier diodes (100 pW/Hz$^{0.5}$) [9]. The NEP value is proportional to the square root of the drain resistance $R_d^{0.5}$ and the inverse responsivity R_v^{-1}. With decreasing the gate swing voltage (V_g - V_{th}), the responsivity becomes larger in the range (V_g - V_{th}) ~ 0.2 V (see Fig. 5), resulting in the decrement of the NEP value. On the other hand, near the threshold condition (V_g - V_{th}) ~ 0, the drain resistance becomes much larger because of the pinch-off, resulting in the increment of the NEP value. As a result, the NEP value becomes minimal around the midpoint (V_g - V_{th}) ~ 0.1 V.

C. *Applications to THz non-destructive sensing*

THz imaging experiment was carried out for an A-DGG HEMT detector using the experimental setup shown in Figs. 6(a) and (b) [9]. The samples under imaging are an IC card and a soap bar. As seen in Fig. 6(c), measured results clearly demonstrate the imaging of hidden substances of circuit/antenna components inside of the IC card and the thickness of the soap bar with a nice contrast and a sub-mm resolution [9].

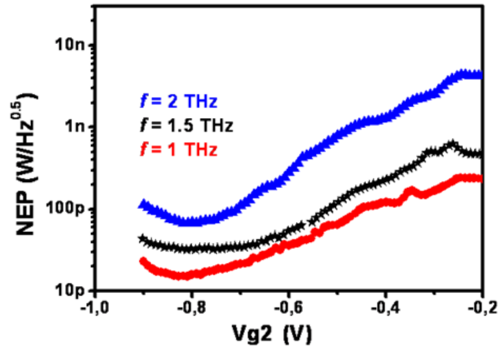

Figure 6. Measured noise equivalent power for sample ACP1 at 1, 1.5, and 2 THz as a function of the gate voltage swing V_{g2} - V_{th2}. The NEP becomes minimum at V_g - V_{th} ～ 0.1 V. (after [8].)

IV. CONCLUSION

Emission and detection of THz radiation using 2D plasmons in semiconductor nano-heterostructures for nondestructive sensing were described. The device structure providing practical emission and detection performances was based on a HEMT and incorporates an A-DGG or AC-DGG structure. Excellent THz emission and detection performances including coherent, monochromatic emission beyond 1-THz range and the record detection responsivity of 6.4 kV/W at 1.5 THz at 300 K were experimentally demonstrated by using InAlAs/InGaAs/InP heterostructure material systems. Finally their applications to nondestructive inspections of objects based on THz imaging are demonstrated. Obtained results encourage us to proceed to further industrialization of these plasmonic THz devices.

ACKNOWLEDGMENT

The authors thank D. Coquillat, Y. Meziani, H. Minamide, and H. Ito for their contributions, and M. Dyakonov, M. S. Shur and S. A. Nikitov for valuable comments and discussion.

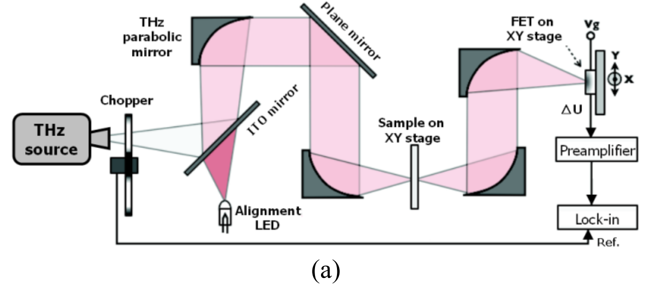

(a)

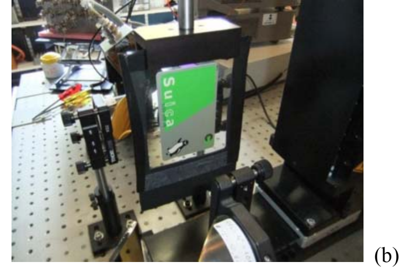

(b)

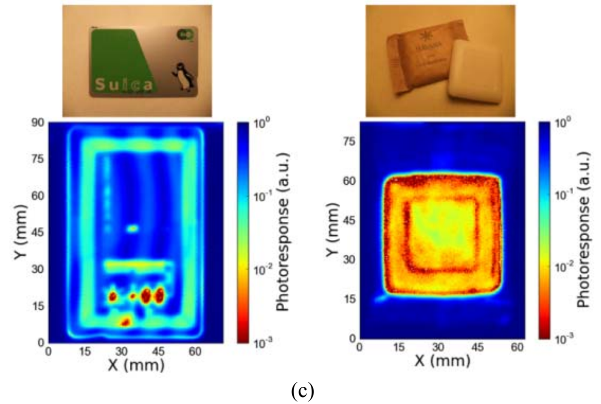

(c)

Figure 5. Imaging setup and results using an InP-based A-DGG HEMT detector. (a) Experimental setup for sub-THz imaging experiments. (b) Photo image of the sample holder of the imaging setup. (c) photo images and THz images measured by using a A-DGG HEMT. Left: an IC card, right: a soap bar. (after [9].)

REFERENCES

[1] M. Dyakonov, M.Shur, "Shallow water analogy for a ballistic field effect transistor: New mechanism of plasma wave generation by dc current," *Phys. Rev. Lett.*, vol. 71, pp. 2465–2468, 1993.

[2] V. Ryzhii, A. Satou, and M.S. Shur, " Transit-time mechanism of plasma instability in high electron mobility transistors," *Phys. Stat. Sol. (a)*, vol. 202, pp. 113-R115, 2005.

[3] M. Dyakonov, and M. Shur, "Detection, mixing, and frequency multiplication of terahertz radiation by two-dimensional electronic fluid," *IEEE Trans. Electron. Dev.*, vol. 43, pp. 1640–1645, 1996.

[4] V. V. Popov et al., "Plasmonic terahertz detection by a double-grating-gate field-effect transistor structure with an asymmetric unit cell," *Appl. Phys. Lett.*, vol. 99, pp. 243504-1-4, 2011.

[5] Otsuji, T., Watanabe, T., Boubanga Tombet, S., Satou, A., Knap, W., Popov, V., Ryzhii, M., and Ryzhii, V., "Emission and detection of terahertz radiation using two-dimensional electrons in III-V semiconductors and graphene," *IEEE Trans. Terahertz Sci. Technol.* **3**, 63-72 (2013).

[6] Otsuji, T., Watanabe, T., El Moutaouakil, A., Karasawa, H., Komori, T., Satou, A., Suemitsu, T., Suemitsu, M., Sano, E., Knap, W., Ryzhii, V., "Emission of terahertz radiation from two-dimensional electron systems in semiconductor nano-and hetero-structure," *J. Infrared Milli. Terahz. Waves* **32**, 629-645 (2011).

[7] T. Watanabe, A. Satou, T. Suemitsu, W. Knap. V.V. Popov, and T. Otsuji, "Plasmonic Terahertz Monochromatic Coherent Emission from an Asymmetric Chirped Dual-Grating-Gate InP-HEMT with a Photonic Vertical Cavities,"CLEO: Conference on Lasers and Electrooptics Dig., CW3K.7, San Jose, CA, USA, June 12, 2013.

[8] Watanabe, T., Boubanga Tombet, S., Tanimoto, Y., Fateev, D., Popov, V., Coquillat, D., Knap, W., Meziani, Y., Wang, Y., Minamide, H., Ito, H., and Otsuji, T., "Ultrahigh sensitive plasmonic terahertz detector based on an asymmetric dual-grating gate HEMT structure," *Solid State Electron.* **78**, 109-114 (2012).

[9] Watanabe, T., Boubanga Tombet, S., Tanimoto, Y., Fateev, D., Popov, V., Coquillat, D., Knap, W., Meziani, Y., Wang, Y., Minamide, H., Ito, H., and Otsuji, T., "InP-and GaAs-based plasmonic high-electron-mobility transistors for room-temperature ultrahigh-sensitive terahertz sensing and imaging," *IEEE Sensors J.* **13**, 89-99 (2013).

[10] Boubanga-Tombet, S., Tanimoto, Y., Watanabe, T., Suemitsu, T., Wang. Y., Minamide, H., Ito, H., Popov, V., and Otsuji, T., "Asymmetric dual-grating gate InGaAs/InAlAs/InP HEMTs for ultrafast and ultrahigh sensitive terahertz detection," DRC: Device Research Conf. Dig., IV.A-10, pp. 169-170, Penn-State, PA, USA, June 19, 2012.